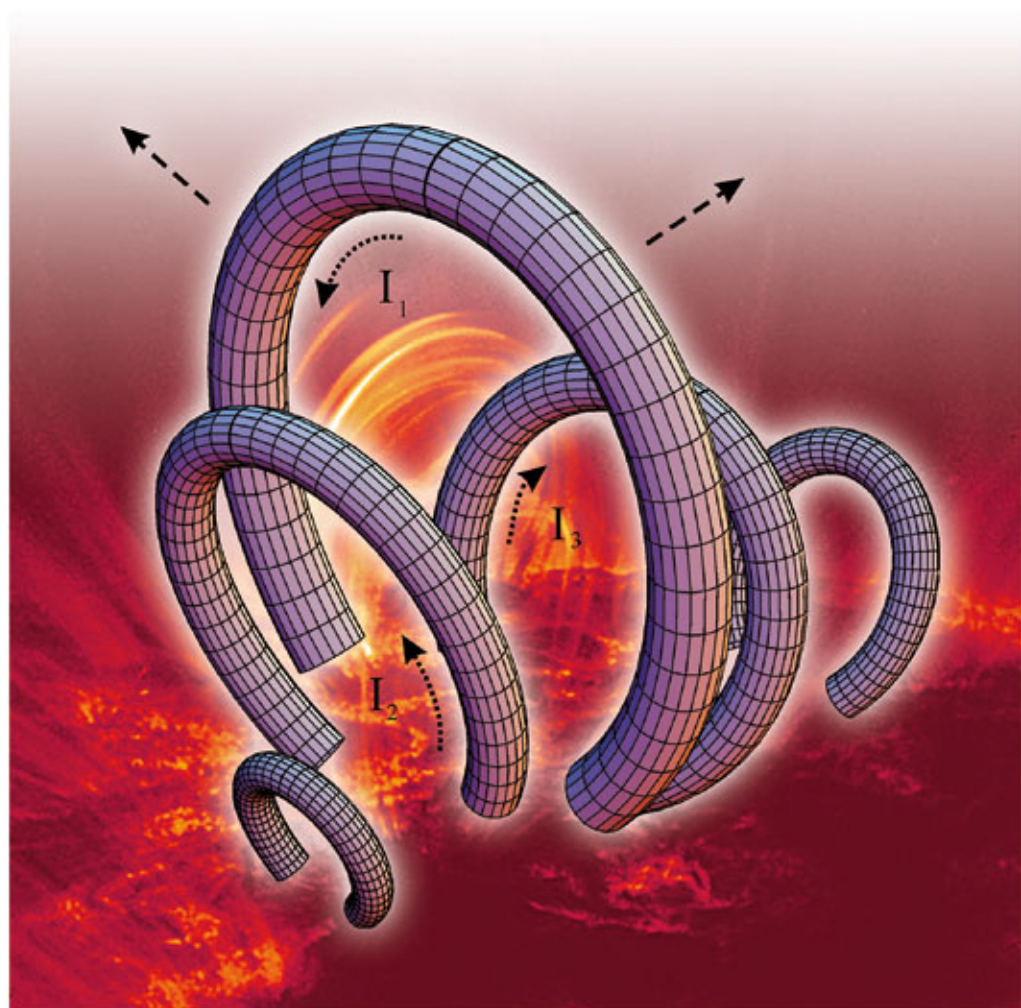


A.V. Stepanov, V.V. Zaitsev,
and V.M. Nakariakov

WILEY-VCH

Coronal Seismology

Waves and Oscillations in Stellar Coronae



*A. V. Stepanov, V. V. Zaitsev,
and V. M. Nakariakov*

Coronal Seismology

Related Titles

Stahler, S. W., Palla, F.

The Formation of Stars

2004

Softcover

ISBN: 978-3-527-40559-6

Foukal, P. V.

Solar Astrophysics

2004

Hardcover

ISBN: 978-3-527-40374-5

Rüdiger, G., Hollerbach, R.

The Magnetic Universe

**Geophysical and Astrophysical Dynamo
Theory**

2004

Hardcover

ISBN: 978-3-527-40409-4

Spitzer, L.

Physical Processes in the Interstellar Medium

1998

Softcover

ISBN: 978-0-471-29335-4

A. V. Stepanov, V. V. Zaitsev, and V. M. Nakariakov

Coronal Seismology

Waves and Oscillations in Stellar Coronae



**WILEY-
VCH**

WILEY-VCH Verlag GmbH & Co. KGaA

The Authors

Prof. Alexander V. Stepanov

Russian Academy of Sciences
Pulkovo Observatory St. Petersburg
Russia Federation
stepanov@gao.spb.ru

Prof. Valery V. Zaitsev

Russian Academy of Sciences
Institute of Applied Physics
Nizhny Novgorod
Russia Federation

Prof. Valery M. Nakariakov

University of Warwick
Department of Physics
Coventry, United Kingdom

Cover picture

© NASA

The Transition Region and Coronal Explorer, TRACE, is a mission of the Stanford-Lockheed Institute for Space Research, and part of the NASA Small Explorer program.

All books published by **Wiley-VCH** are carefully produced. Nevertheless, authors, editors, and publisher do not warrant the information contained in these books, including this book, to be free of errors. Readers are advised to keep in mind that statements, data, illustrations, procedural details or other items may inadvertently be inaccurate.

Library of Congress Card No.: applied for

British Library Cataloguing-in-Publication Data

A catalogue record for this book is available from the British Library.

Bibliographic information published by the Deutsche Nationalbibliothek

The Deutsche Nationalbibliothek lists this publication in the Deutsche Nationalbibliografie; detailed bibliographic data are available on the Internet at <http://dnb.d-nb.de>.

© 2012 Wiley-VCH Verlag & Co. KGaA, Boschstr. 12, 69469 Weinheim, Germany

All rights reserved (including those of translation into other languages). No part of this book may be reproduced in any form – by photoprinting, microfilm, or any other means – nor transmitted or translated into a machine language without written permission from the publishers. Registered names, trademarks, etc. used in this book, even when not specifically marked as such, are not to be considered unprotected by law.

Typesetting Laserwords Private Limited, Chennai, India

Printing and Binding Markono Print Media Pte Ltd, Singapore

Cover Design Grafik-Design Schulz, Fußgönheim

Printed in Singapore

Printed on acid-free paper

Print ISBN: 978-3-527-40994-5

ePDF ISBN: 978-3-527-64601-2

oBook ISBN: 978-3-527-64598-5

ePub ISBN: 978-3-527-64600-5

mobi ISBN: 978-3-527-64599-2

Contents

Preface IX

1	Introduction	1
1.1	Magnetic Loops and Open Flux Tubes as Basic Structural Elements in Solar and Stellar Coronae	1
1.2	Data of Observations and Types of Coronal Loops	2
1.3	The MHD Approach for Coronal Plasma	5
	References	8
2	Coronal Magnetic Loop as an Equivalent Electric Circuit	9
2.1	A Physical Model of an Isolated Loop	10
2.2	The Formation of Magnetic Tubes by Photospheric Convection	12
2.3	The Structure of the Coronal Part of a Flux Tube	18
2.4	Diagnostics of Electric Currents	21
2.4.1	“Warm” Loops	21
2.4.2	“Hot X-ray” Loops	22
2.4.2.1	Flare Magnetic Loops	23
2.5	The Equivalent Electric Circuit	25
2.6	Inductive Interaction of Magnetic Loops	29
2.7	Waves of Electric Current in Arcades of Coronal Magnetic Loops	30
2.8	Magnetic Loops above Spots	33
	References	36
3	Resonators for MHD Oscillations in Stellar Coronae	39
3.1	Eigenmodes of Coronal Loops: The Plasma Cylinder Approach and the Dispersion Equation	40
3.1.1	Trapped Modes	43
3.1.1.1	Global Sausage Mode	45
3.1.1.2	Global Kink Mode	45
3.1.2	Leaky Modes	46
3.1.2.1	Sausage Mode	46
3.1.2.2	Kink Modes	51
3.1.3	Ballooning Modes	53

3.2	MHD Resonator at $\sim 1R_{\odot}$ in the Solar Corona	54
3.3	Excitation Mechanisms for Loop Oscillations	57
3.3.1	External Triggers	57
3.3.2	Parametric Excitation of Loop Oscillations by p-Modes	59
3.3.3	Internal Excitation	60
3.3.3.1	The Excitation of the Sausage Mode by Instantaneous Energy Release	61
3.3.3.2	The Excitation of the Global Kink Mode by Chromosphere Evaporation	62
3.3.3.3	The Excitation of the Sausage Mode by High-Energy Protons under the Bounce-Resonance Condition	63
	References	64
	Further Reading	66
4	Propagating MHD Waves in Coronal Plasma Waveguides	67
4.1	MHD Waves in Vertical Coronal Magnetic Flux Tubes	68
4.1.1	Effects of Stratification	69
4.2	Propagating Waves in Coronal Loops	74
4.2.1	Propagating Compressible Waves in Coronal Loops	74
4.2.2	Transverse Waves in Coronal Loops	78
4.3	Waves in Coronal Jets	80
4.4	Evolution of Short-Wavelength, Fast Magnetoacoustic Waves	82
4.5	Alfvén Wave Phase Mixing	87
4.5.1	Damping of Alfvén Waves because of Phase Mixing	88
4.5.2	Enhanced Nonlinear Generation of Oblique Fast Waves by Phase-Mixed Alfvén Waves	89
	References	91
5	Prominence Seismology	93
5.1	Prominence Models	93
5.2	Prominence Oscillations	95
5.3	The Heating Effect	97
5.4	Nonlinear Oscillations: Dynamical Modes	99
5.5	Flare Processes in Prominences	108
5.6	Stellar and Interstellar Prominences	109
	References	111
6	The Coronal Loop as a Magnetic Mirror Trap	113
6.1	Particle Distribution in a Coronal Loop	113
6.1.1	Gyrosynchrotron Emission from a Flaring Loop	116
6.2	Kinetic Instabilities in a Loop	118
6.2.1	A Loop as an Electron Cyclotron Maser	118
6.2.2	The Plasma Mechanism of the Radio Emission from Coronal Loops	119
6.2.3	Instabilities of Whistlers and Small-Scale Alfvén Waves	123

6.3	The Fine Structure of Radio Emission from Coronal Loops	125
6.3.1	Sudden Reductions	126
6.3.2	Zebra Pattern	126
6.3.3	Diagnostics of Coronal Plasma Using the Fine Structure of Radio Emission	129
	References	129
7	Flaring Events in Stellar Coronal Loops	131
7.1	Particle Acceleration and Explosive Joule Heating in Current-Carrying Loops	131
7.1.1	Where Is the Acceleration Region Located?	132
7.1.2	Large-Scale Electric Fields in Flare Loops	133
7.1.2.1	The Charge-Separation Electric Field	134
7.1.2.2	Inductive Electric Field	136
7.1.3	The Impulsive and Pulsating Modes of Acceleration	138
7.1.4	The Current of Accelerated Electrons (Colgate's Paradox)	140
7.1.5	Explosive Joule Energy Release. The Role of Flute Instability and Cowling Conductivity	140
7.2	The Kinematics of Energetic Particles in a Loop and the Consequent Radiation	143
7.2.1	Diffusion Regimes of Accelerated Particles in Coronal Loops	145
7.2.2	Consequences of the Strong Diffusion of Energetic Particles	149
7.2.2.1	Turbulent Propagation of Fast Electrons in a Loop	149
7.2.2.2	Turbulent Propagation of Superthermal Ions: the Absence of Linear Polarization in $H\alpha$ Emission of a Solar Flare	155
7.2.2.3	Time Delays in Hard X-Ray and γ -Ray Emission	158
7.2.2.4	Transformation of Energetic Particle Spectra in a Coronal Loop	160
	References	161
	Further Reading	163
8	Stellar Coronal Seismology as a Diagnostic Tool for Flare Plasma	165
8.1	Modulation of Flaring Emission by MHD Oscillations	165
8.1.1	Modulation of Gyrosynchrotron Emission	166
8.1.2	Modulation of Plasma Radiation	167
8.1.3	Modulation of the Electron Precipitation Rate	168
8.2	Global Sausage Mode and Diagnostics of the Solar Event of 12 January 2000	169
8.3	Dissipative Processes in Coronal Loop for MHD Modes	171
8.4	The Stellar Flare Plasma Diagnostics from Multiwavelength Observations Stellar Flares	172
8.4.1	Pulsations in the Optical Range (U,B) in an EV Lac Flare	173
8.4.2	Quasi-Periodic Oscillations (QPOs) from EQ Peg	174
8.4.3	Soft X-Ray Pulsations from a Flare of AT Mic	176
8.5	Diagnostics of Electric Currents in Stellar Atmospheres	177

8.5.1	Observational Evidence for Energy Accumulation and Dissipation in Coronal Magnetic Loop	178
8.5.2	Pulsating Microwave Emission from AD Leo	181
	References	183
9	Heating Mechanisms in Stellar Coronae	185
9.1	Wave Heating	186
9.1.1	Parametric Excitation of Acoustic Oscillations	188
9.1.2	The Energy of Acoustic Oscillations	189
9.1.3	Acoustic Wave Heating Function	191
9.1.4	Thermal Balance in a Coronal Magnetic Loop	192
9.1.5	Hot X-Ray Loops in the Solar Corona	194
9.1.6	Magnetic Loops in Late-Type Stars	195
9.2	Ohmic Dissipation of Electric Currents	196
9.3	Heating by Microflares	199
	References	203
10	Loops and QPOs in Neutron Stars and Accretion Disk Coronae	205
10.1	The Origin of Fast QPOs from Magnetars and Diagnostics of Magnetar Corona	205
10.1.1	A Brief Overview of the Existing Models	206
10.1.2	An Equivalent Electric RLC Circuit	208
10.1.3	The Flare of SGR 1806-20 on 27 December 2004	209
10.1.4	Excitation of High-Frequency Current Oscillations of the Current in Coronal Loop	210
10.2	Coronae of Accretion Disks	212
10.2.1	Accretion Disk Corona of Cyg X-1	213
10.2.2	QPOs in Accretion Disks	215
	References	215
11	Conclusions	217
	References	218
	Index	219

Preface

Wave and oscillatory phenomena, which are intrinsically inherent in the activity of solar and stellar coronae, present the subject of *coronal seismology* – a new rapidly developing branch of astrophysics. The philosophy of this novel method of remote diagnostics of plasma parameters is analogous to the study of the Earth's interior by surface and body waves, *geoseismology*. In solar and stellar physics, a similar technique for probing of the interiors, *helio-* and *asteroseismology*, is successfully applied. Moreover, the observational detection of waves and oscillations in accretion disks recently gave rise to the topic of *diskoseismology*. Likewise, magnetoseismology, the diagnostics of the Earth's (and, potentially, planetary) magnetospheres with magnetohydrodynamic waves and oscillations, is another successful manifestation of this technique.

Hundreds of papers and reviews as well as national and international meetings are devoted now to the current problems in the field of the coronal seismology. Flares, charged particle acceleration and emission, plasma heating, prominence dynamics, and coronal mass ejections are related to the magnetic structures of active regions of the stars. Numerous ground- and space-borne observations provide evidence that magnetic flux tubes and loops, being a typical structure of solar and stellar coronae, act as waveguides and resonators for magnetohydrodynamical (MHD) waves and oscillations. Moreover, modern view suggests that coronae of accretion disks and neutron stars also consist of magnetic loops. Waves and oscillations in open and closed magnetic structures modulate solar and stellar emission in various wave bands. Hence, coronal seismology can provide a good diagnostic tool for flare plasma as well as for energy transfer and energy transformation in solar and stellar atmospheres. More opportunities in the coronal seismology were made more than a decade ago with the use of space missions: the Solar and Heliospheric Observatory and Transition Region and Coronal Explorer. New good chances for coronal plasma diagnostics open now with the Solar Dynamic Observatory and Solar Terrestrial Relations Observatory.

This book is devoted to the successive exposition of the main problems of the coronal seismology. Two approaches are mainly used for the interpretation of the wave and oscillatory phenomena in solar and stellar coronae. The first approach represents the coronal magnetic loops and flux tubes as resonators and waveguides for MHD oscillations and waves. The second one describes the coronal loop in

terms of an equivalent electric circuit with the effective resistance, inductance, and capacitance. Both these approaches complement one another effectively in the process of diagnostics of coronal plasma. Because waves and oscillations cause quasi-periodic modulations of plasma parameters of coronal magnetic structures, the emission mechanisms from coronal structures of both thermal and nonthermal origins should be studied in this context. Most pronounced phase of quasi-periodic pulsations is in the course of flaring event. Hence, the flare plasma heating and charged particle acceleration are also the subjects of this book.

It should be noted that the author's views are biased by their own preferences and interests. However, they tried to address wider problems of the coronal seismology. Sometimes the main formulas and notations are repeated in various chapters for the reader's convenience.

December 2011

A. V. Stepanov
V. V. Zaitsev
V. M. Nakariakov

1

Introduction

Uchida [1], who suggested the idea of plasma and magnetic field diagnostics in the solar corona on the basis of waves and oscillations in 1970, and Rosenberg [2], who first explained the pulsations in type IV solar radio bursts in terms of the loop magnetohydrodynamic (MHD) oscillations, can be considered to be pioneers of coronal seismology.

Various approaches have been used to describe physical processes in stellar coronal structures: kinetic, MHD, and electric circuit models are among them. Two main models are presently very popular in coronal seismology. The first considers magnetic flux tubes and loops as wave guides and resonators for MHD waves and oscillations, whereas the second describes a loop in terms of an equivalent electric (RLC) circuit. Several detailed reviews are devoted to problems of coronal seismology (see, i.e., [3–7]). Recent achievements in the solar coronal seismology are also referred in *Space Sci. Rev.* vol. 149, No. 1–4 (2009). Nevertheless, some important issues related to diagnostics of physical processes and plasma parameters in solar and stellar flares are still insufficiently presented in the literature. The main goal of the book is the successive description and analysis of the main achievements and problems of coronal seismology.

There is much in common between flares on the Sun and on late-type stars, especially red dwarfs [8]. Indeed, the timescales, the Neupert effect, the fine structure of the optical, radio, and X-ray emission, and the pulsations are similar for both solar and stellar flares. Studies of many hundreds of stellar flares have indicated that the latter display a power-law radiation energy distribution, similar to that found for solar flares. Thus, we can use the solar–stellar analogy to study flaring stars.

The next goal of this book is to illustrate the efficiency of coronal seismology as a diagnostic tool for the analysis of stellar flares.

1.1

Magnetic Loops and Open Flux Tubes as Basic Structural Elements in Solar and Stellar Coronae

Magnetic loops constitute the basic structural element in the coronae of the Sun and late-type stars [9–11]. They play an important role in solar activity. Observations

made with *Skylab*, Solar and Heliospheric Observatory (SOHO), *Yohkoh*, Reuven Ramaty High-Energy Solar Spectroscopic Imager (RHESSI), Transition Region and Coronal Explorer (TRACE), Complex Orbital Near-Earth Observations of Activity of the Sun – Photon (CORONAS–F), *Hinode*, Solar Dynamic Observatory (SDO) space missions, as well as with large optical telescopes Vacuum Tower Telescope (VTT), and radio telescopes (Very Large Array (VLA), Siberian Solar Radio Telescope (SSRT), NoRH (Nobeyama Radioheliograph)) have shown that solar flares originate in coronal loops [3, 12]. Eruptive prominences and coronal transients result in giant coronal mass ejections (CMEs) and also frequently display the loop shape [13]. The flaring activity of dMe-stars and close binaries is also spawned by the energy release in magnetic loops [9, 14, 15]. In some late-type stars, magnetic spots cover up to 70–80% of the surface, whereas solar spots occupy $\sim 0.04\%$ of the photosphere. This implies that, in fact, loops form the magnetic structure of stellar coronae. In addition, loops are typical for the magnetic structure of the atmospheres of accretion disks, young stellar objects, and neutron stars [16–19]. Owing to space-borne observations and advances in the physics of the loops, some progress has been recently made in finding a solution for the problem of the origin of coronal loops. Alfvén and Carlqvist [20] have suggested that a flaring loop can be considered to be an equivalent electric circuit. This phenomenological approach was nevertheless very productive in understanding the energy pattern of flare processes. The description of the loops in terms of resonators and wave guides for MHD waves explains various kinds of modulations of stellar flare emissions and serves as a diagnostic tool for the flare plasma. The concept of a coronal loop as a magnetic mirror trap for energetic particles makes it possible to efficiently describe particle dynamics and peculiarities of emission generated by energetic particles.

Open magnetic structures – the flux tubes – are wave guides for MHD waves, which make them important channels of energy transfer from one part of the stellar atmosphere to another, from the photosphere and chromosphere to the corona, and further to the solar and stellar wind. Similar to magnetic loops, the flux tubes provide a necessary link in the mechanism of coronal heating. Flux tubes are exemplified by solar spicules, which are energy/mass bridges between the dense and dynamic photosphere and the tenuous hot solar corona [21].

Prominence dynamics and oscillations also present important subjects for coronal seismology [22, 23] since prominences play a crucial role both in triggering flares [24, 25] and in CME's origin [26]. Therefore, the study of ballooning instability presents a very important point in the context of flaring and CME's activity.

1.2

Data of Observations and Types of Coronal Loops

The corona of the Sun (a main-sequence G2 star) in its active phase consists predominantly of magnetic loops filled with comparatively dense and hot plasma, which is observed in soft X rays and constitutes an essential part of the total mass of the corona. The presence of magnetic loops indicates the complexity

of the subphotospheric magnetic field, which is most likely linked to convective motions of the photosphere matter. Observations indicate that there are at least five morphologically distinct types of loops present in the solar atmosphere (see, i.e., [27, 28]):

- 1) **Loops connecting different active regions.** Their lengths reach 700 000 km, the plasma temperature in such loops is $(2-3) \times 10^6$ K, and the density is about 10^9 cm^{-3} . The loop footpoints are located in islands of the strong magnetic field on the periphery of active regions. The characteristic lifetime of such loops is about one day.
- 2) **Loops in quiescent regions.** They do not connect active regions; their lengths are the same as those of the previous types of loops. Their temperature, however, is somewhat lower, within the interval $(1.5-2.1) \times 10^6$ K, while the density is in the range $(2-10) \times 10^8 \text{ cm}^{-3}$.
- 3) **Loops in active regions.** Their lengths span from 10 000 to 100 000 km and temperature and density are within the intervals $10^4-2.5 \times 10^6$ K and $(0.5-5.0) \times 10^9 \text{ cm}^{-3}$, respectively.
- 4) **Post-flare loops.** They commonly connect footpoints of two-ribbon flares, and display lengths of 10 000–100 000 km, temperature $10^4-4 \times 10^6$ K, and density up to 10^{11} cm^{-3} .
- 5) **Single-flare loops.** These are separate loops, in which flare energy is released. Hard X-ray bursts last for about a minute and are the most pertinent feature of such flares. In soft X rays, these loops are characterized by small volumes and low heights. The loops are 5000–50 000 km in length, their temperature is less than 4×10^7 K, and their plasma density reaches 10^{12} cm^{-3} [12].

Closed magnetic structures resembling coronal loops also exist in stars of other types. Data obtained with *Einstein*, *ROSAT* (Röntgensatellit), and *XMM-Newton* (XMM stands for X-ray multimirror mission) space missions indicate that virtually all stars on the Hertzsprung–Russell diagram possess hot coronae with temperatures ranging between 10^7 and 10^8 K [29–31]. They are not confined gravitationally, which implies the presence of magnetic fields. Of special interest are late-type stars, particularly dMe red dwarfs, which display high flare activity and represent nearly 80% of the total number of stars in the Galaxy and in its close neighborhood. Although red dwarfs are morphologically similar to the Sun, especially in their radio-wavelength radiation (the slowly varying component, rapidly drifting bursts, sudden reductions, spike bursts, and quasi-periodical pulsations [15, 32]), these objects present some peculiarities, which stem from the high activity of their coronae.

First, note the high brightness temperature of the “quiescent” radio emission of dMe-stars (up to 10^{10} K), which cannot be described in terms of thermal coronal plasma with the temperature 10^7-10^8 K. This radiation is commonly interpreted as gyrosynchrotron emission of nonthermal electrons abundant in the coronae of red dwarfs. The coexistence of the hot plasma and subrelativistic particles is also suggested by the correlation between the radio and soft X-ray emission over six orders of magnitude in intensity [33]. This phenomenon is not observed in the solar corona. In the quiescent state, the corona of the Sun does not host a sufficient

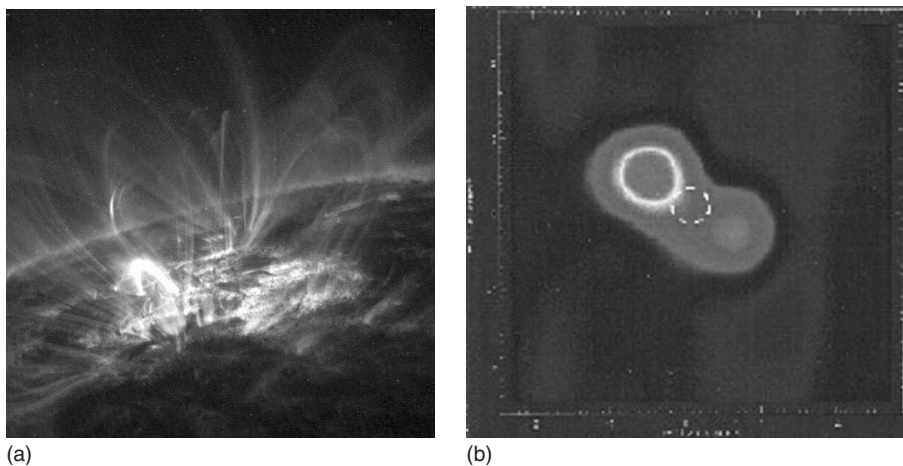


Figure 1.1 (a) Coronal magnetic loops of an active region on the Sun observed with the space laboratory TRACE in the ultraviolet range, $\lambda = 171 \text{ \AA}$ [11]. A hot flare loop stands out sharply. (b) Radio map of UV Cet on the wavelength of 3.6 cm obtained with VLBA (very long baseline array) and VLA (very large array). The dashed line marks the optical disk of the star [10].

Table 1.1 Parameters of coronal flare loops.

Parameter	The Sun	Red draft UV Ceti	Close binary stars	
			RS CVn	Algol
Length (cm)	$(1-10) \times 10^9$	$2 \times 10^9 - 3 \times 10^{11}$	$(5-10) \times 10^{10}$	$(2-6) \times 10^{11}$
Lateral size (cm)	$(1-5) \times 10^8$	$10^8 - 3 \times 10^9$	—	—
Plasma density n (cm^{-3})	$10^9 - 10^{12}$	$10^{10} - 10^{12}$	$10^8 - 10^{10}$	$10^9 - 10^{12}$
Plasma temperature T (K)	$10^6 - 10^7$	$3 \times 10^6 - 10^8$	$(3-9) \times 10^7$	$(3-7) \times 10^7$
Magnetic field induction B (G)	$10^2 - 10^3$	$3 \times 10^2 - 10^3$	$(0.3-6) \times 10^2$	$(1-5) \times 10^2$
Emission measure (EM) (cm^{-3})	$10^{47} - 10^{50}$	$10^{50} - 10^{53}$	$10^{53} - 10^{55}$	$10^{52} - 10^{54}$

number of high-energy particles, and the brightness temperature of solar radio emission does not exceed 10^6 K.

Second, the difference is manifested in the extremely high brightness temperature of flare radio emission of red dwarves, sometimes exceeding 10^{16} K, which is three to four orders of magnitude higher than that of the most powerful radio bursts in the Sun. This suggests the presence of an efficient coherent (maser) mechanism of emission from stellar coronae. Moreover, in red dwarfs, radio flares can frequently occur independently of optical flares.

Third, the sizes of loops on the Sun and red dwarves are different [9, 10]. As a rule, the length of the solar loops, with the exception of trans-equatorial ones, is substantially smaller than that of the solar radius (Figure 1.1a). On red dwarves, the size of magnetic loops can be comparable to the stellar radii or can exceed them by a few factors (Figure 1.1b). The magnetic field in stellar loops can exceed that in solar loops by an order of magnitude.

Table 1.1 presents parameters of flare loops on the Sun and late-type stars derived from multiwavelength (optical, radio, and X-ray) observations and various diagnostic methods.

1.3

The MHD Approach for Coronal Plasma

In our study of magnetic structures in coronal plasma and their evolution, we frequently use MHD approximation. It includes Maxwell equations, generalized Ohm's law, and also equations of motion and continuity of mass, the energy equation, and the gas equation of state. In MHD approximation, it is common to take the simplified Maxwell equations, without taking into account the bias current, and also the simplified form of the Ohm's law in the approximation of isotropic conductivity of plasma. For a number of problems of coronal seismology, such approximations appear to be insufficient, and more general equations are used. In addition to that, when the dynamics and radiation of fast particles in coronal magnetic loops are analyzed, the kinetic equation for the velocity distribution of particles should be used (see, for example, Chapters 6 and 7). Below, we present the basic equations of magnetic hydrodynamics in their generalized form, which is applied further on. For the sake of convenience, we repeatedly reproduce these equations along with the explanation for the previously used notation in different sections.

The *Maxwell equations* in the Gaussian system of units (cgs) may be written in the form

$$\text{rot} \vec{B} = \frac{4\pi}{c} \mu \vec{j} + \frac{1}{c} \mu \varepsilon \frac{\partial \vec{E}}{\partial t} \quad (1.1)$$

$$\text{rot} \vec{E} = -\frac{1}{c} \frac{\partial \vec{B}}{\partial t} \quad (1.2)$$

$$\text{div} \vec{B} = 0 \quad (1.3)$$

$$\text{div} \vec{E} = \frac{1}{\varepsilon} 4\pi \rho_e \quad (1.4)$$

Here, the magnetic induction \vec{B} and magnetic field \vec{H} are related as follows: $\vec{B} = \mu \vec{H}$, while the electric field \vec{E} may be expressed through electric induction: $\vec{E} = \vec{D}/\varepsilon$, where μ and ε are magnetic and dielectric permeabilities. For coronal plasma, μ and ε are usually taken to be equal to their values in vacuum; in the Gaussian system of units (cgs), we further assume $\mu = \varepsilon = 1$. In Eqs. (1.1)

and (1.4), \vec{j} and ρ_e are the density of the electric current and electric charge, respectively.

The *generalized Ohm's law* follows the “three-fluid” model for electrons, ions, and neutral atoms; it connects the electric current with the velocity of the center of mass, and also with the electric and magnetic fields. When the inertia of electrons is neglected, the generalized Ohm's law is written as follows:

$$\vec{E} + \frac{1}{c} \vec{V} \times \vec{B} = \frac{\vec{j}}{\sigma} + \frac{\vec{j} \times \vec{B}}{enc} + \frac{\vec{f}_e}{en} + F \frac{[\vec{f}_a \times \vec{B}]}{cnm_i v'_{ia}} - \frac{F^2 \rho}{cnm_i v'_{ia}} \left[\frac{d\vec{V}}{dt} \times \vec{B} \right] \quad (1.5)$$

Here, $\rho = n_a m_a + n_e m_e + n_i m_i$ is the plasma density, $p = p_a + p_e + p_i$ is its pressure, $\vec{V} = \left(\sum_k n_k m_k \vec{V}_k \right) / \left(\sum_k n_k m_k \right)$ is the average velocity of plasma motion, $k = a, i, e$ (a, atoms; i, ions; and e, electrons), $\sigma = \frac{ne^2}{m_e(v'_{ei} + v'_{ea})}$ is the Coulomb (Spitzer) conductivity, $F = \rho_a / \rho$ is the relative density of neutrals, ν_{kl} is the frequency of collisions between particles of k and l types, $\nu'_{kl} = [m_l / (m_k + m_l)] \nu_{kl}$ is the effective frequency of collisions, $n_i = n_e = n$, $\vec{f}_e = -\text{grad } p_e$, $\vec{f}_a = -\text{grad } p_a + n_a m_a \vec{g}$, and \vec{g} is the gravitational acceleration. Two last summands in the right-hand part of Eq. (1.5) take into account dissipation related to ion–atom collisions. Under the conditions in the chromospheres and even of the corona, this dissipation frequently appears to be more efficient than that caused by Spitzer conductivity σ .

The induction equation. Excluding the electric field from Eq. (1.5) with the use of Eq. (1.2), we obtain the following equation for magnetic induction:

$$\begin{aligned} \frac{\partial \vec{B}}{\partial t} &= \eta \nabla^2 \vec{B} + \text{rot} [\vec{V} \times \vec{B}] + \frac{F^2 \rho}{n_i m_i v'_{ia}} \text{rot} \left[\frac{d\vec{V}}{dt} \times \vec{B} \right] \\ &\quad - \frac{F}{n_i m_i v'_{ia}} \text{rot} [\vec{f}_a \times \vec{B}] - \frac{1}{en_i} \text{rot} [\vec{j} \times \vec{B}] \end{aligned} \quad (1.6)$$

where $\eta = c^2 / 4\pi\sigma$ is the magnetic viscosity. Frequently, only the first two terms in the right-hand part of the induction Eq. (1.6) are taken into account, which correspond to the simplest form of the Ohm's law

$$\vec{j} = \sigma \left(\vec{E} + \frac{1}{c} \vec{V} \times \vec{B} \right) \quad (1.5a)$$

This form of Ohm's law may be applied, for instance, in the case of totally ionized plasma ($\vec{f}_a = 0$), provided the Ampere force becomes zero ($\vec{j} \times \vec{B} = 0$, the so-called force-free approximation). In a more general case, for example, in the lower chromosphere or in the prominence, plasma is partly ionized, and the anisotropy of conductivity becomes essential. Therefore, the more general induction Eq. (1.6) should be used.

Equations of plasma. The induction Eq. (1.6) indicates that the behavior of the magnetic field is related to the motion of plasma, since in this equation some summands contain the matter velocity. In turn, the motion of plasma is specified

by the continuity equation, the equation of motion, and the energy equation:

$$\frac{\partial \rho}{\partial t} + \text{div}(\rho \vec{V}) = 0 \quad (1.7)$$

$$\rho \frac{D\vec{V}}{Dt} = -\nabla p + \frac{1}{c} \vec{j} \times \vec{B} + \rho \vec{g} \quad (1.8)$$

$$\frac{\rho^\gamma}{\gamma - 1} \frac{D}{Dt} \left(\frac{p}{\rho^\gamma} \right) = -Q \quad (1.9)$$

In Eqs. (1.8) and (1.9), $D/Dt = \partial/\partial t + (\vec{v} \cdot \nabla)$ means the convective derivative that specifies time variations of parameters related to plasma motion. In Eq. (1.9), $\gamma = C_P/C_V$ is the ratio between specific heat capacities and Q is the function equal to the difference between the energy loss and energy inflow rates per unit volume of plasma. The energy loss commonly consists of the thermal conductivity and radiative losses. In coronal magnetic fields, the thermal conductivity across the magnetic field may commonly be neglected. In addition to that, in the optically thin part of the atmosphere ($T \geq 2 \times 10^4$ K in the chromosphere and in the corona), the radiative losses do not depend on the radiation intensity, which results in simplification of the radiative loss function. If along with that the energy inflow rate is specified by dissipation of electric currents, the function Q may be presented as follows:

$$Q = -\frac{1}{A} \frac{d}{ds} \left(\kappa_e \frac{dT}{ds} A \right) + n_e n_H \chi(T) - \left(\vec{E} + \frac{1}{c} \vec{V} \times \vec{B} \right) \vec{j} \quad (1.10)$$

Here, $A(s)$ is the cross section of the force tube related to the magnetic field, s is the coordinate along the tube, and $\kappa_e = 0.92 \times 10^{-6} \text{ erg cm}^{-1} \text{ K}^{-7/2}$ is the coefficient of thermal conductivity along the magnetic field,

$$\begin{aligned} \chi(T) &\approx 10^{-21.85} \quad (10^{4.3} \leq T \leq 10^{4.6} \text{ K}) \\ &\approx 10^{-31} T^2 \quad (10^{4.6} \leq T \leq 10^{4.9} \text{ K}), \\ &\approx 10^{21.2} \quad (10^{4.9} \leq T \leq 10^{5.4} \text{ K}) \\ &\approx 10^{-10.4} T^{-2} \quad (10^{5.4} \leq T \leq 10^{5.75} \text{ K}) \\ &\approx 10^{-21.94} \quad (10^{5.75} \leq T \leq 10^{6.3} \text{ K}) \\ &\approx 10^{-17.73} T^{-2/3} \quad (10^{6.3} \leq T \leq 10^7 \text{ K}) \end{aligned} \quad (1.11)$$

is the temperature function, the values of which are presented, for example, in Ref. [34]; n_H is the number of hydrogen atoms in the unit volume (for totally ionized plasma, $n_H = n_e$). The last summand in Eq. (1.10) is determined by taking Ohm's law into account (Eq. (1.5)). Within the temperature interval $10^5 \text{ K} < T < 10^7 \text{ K}$, a possible approximation for the radiative loss function is $\chi(T) = \chi_0 T^{-1/2} \text{ erg cm}^3 \text{ s}^{-1}$, where $\chi_0 = 10^{-19}$ [27].

The connection between the pressure and the density is specified by the equation of state; for ideal gas,

$$p = nk_B T \quad (1.12)$$

where $n = n_e + n_i + n_a$ is the total number of particles in unit volume and k_B is the Boltzmann's constant. Different versions of the equations used in MHD approximation are considered in more detail in the monograph by Priest [27].

References

1. Uchida, Y. (1970) *Publ. Astron. Soc. Jpn.*, **22**, 341.
2. Rosenberg, H. (1970) *Astron. Astrophys.*, **9**, 159.
3. Aschwanden, M.J., Poland, A.I., and Rabin, D. (2001) *Ann. Rev. Astron. Astrophys.*, **39**, 175.
4. Aschwanden, M.J. (2003) NATO Advances Research Workshop, NATO Science Series II, p. 22.
5. Nakariakov, V.M. and Verwichte, E. (2005) *Living Rev. Sol. Phys.* Coronal waves and oscillations, **2**, No 3, pp. 3–65
6. Nakariakov, V.M. and Stepanov, A.V. (2007) *Lect. Notes Phys.*, **725**, 221.
7. Zaitsev, V.V. and Stepanov, A.V. (2008) *Phys. Usp.*, **51**, 1123.
8. Gershberg, R.E. (2005) *Solar-Type Activity in Main-Sequence Stars*, Springer, Berlin, Heidelberg.
9. Bray, R.J., Cram, L.E., Durrant, C.J., and Loughhead, R.E. (1991) *Plasma Loops in the Solar Corona*, Cambridge University Press.
10. Benz, A., Conway, J., and Güdel, M. (1998) *Astron. Astrophys.*, **331**, 596.
11. Schrijver, C.J., Title, A.M., Berger, T.E., Fletcher, L. *et al.* (1999) *Sol. Phys.*, **187**, 261.
12. Sakai, J.-I. and de Jager, C. (1996) *Space Sci. Rev.*, **77**, 1.
13. Plunkett, S.P., Vourlidas, A., Šimberová, S., Karlický, M. *et al.* (2000) *Sol. Phys.*, **194**, 371.
14. Lestrade, J.F. (1988) *Astrophys. J.*, **328**, 232.
15. Bastian, T.S., Bookbinder, J.A., Dulk, G.A., and Davis, M. (1990) *Astrophys. J.*, **353**, 265.
16. Galeev, A.A., Rosner, R., Serio, S., and Vaiana, G.S. (1981) *Astrophys. J.*, **243**, 301.
17. Kuijpers, J. (1995) *Lect. Notes Phys.*, **444**, 135.
18. Feigelson, E.D. and Montmerle, T. (1999) *Ann. Rev. Astron. Astrophys.*, **37**, 363.
19. Beloborodov, A.M. and Thompson, C. (2007) *Astrophys. J.*, **657**, 967.
20. Alfvén, H. and Carlqvist, P. (1967) *Sol. Phys.*, **1**, 220.
21. Zaqarashvili, T.V. and Erdelyi, R. (2009) *Space Sci. Rev.*, **149**, 355.
22. Oliver, R. (2009) *Space Sci. Rev.*, **149**, 175.
23. Tripathi, D., Isobe, H., and Jain, R. (2009) *Space Sci. Rev.*, **149**, 283.
24. Pustyl'nik, L.A. (1974) *Sov. Astron.*, **17**, 763.
25. Zaitsev, V.V., Urpo, S., and Stepanov, A.V. (2000) *Astron. Astrophys.*, **357**, 1105.
26. Gopalswamy, N. (2006) *Space Sci. Rev.*, **124**, 145.
27. Priest, E.R. (1982) *Solar Magnetohydrodynamics*, D. Reidel Publishing Company, Dordrecht.
28. Aschwanden, M.J. (2005) *Physics of the Solar Corona. An Introduction with Problems and Solutions*, Springer.
29. Haisch, B.M. (1983) in *Activity in Red-Dwarf Stars X-ray Oscillations of Stellar Flares* (eds P.B. Birne and M. Rodono), Reidel, p. 255–268.
30. Schmitt, J.H.M.M., Collura, A., Sciortino, S., Vaiana, G.S. *et al.* (1990) *Astrophys. J.*, **365**, 704.
31. Mullan, D.J., Mathioudakis, M., Bloomfield, D.S., and Christian, D.J. (2006) *Astrophys. J. Suppl.*, **164**, 173.
32. Stepanov, A.V., Kliem, B., Zaitsev, V.V. *et al.* (2001) *Astron. Astrophys.*, **374**, 1072.
33. Güdel, M. and Benz, A.O. (1993) *Astrophys. J.*, **405**, L63.
34. Rosner, R., Tucker, G.S., and Vaiana, R. (1978) *Astrophys. J.*, **220**, 643.

2

Coronal Magnetic Loop as an Equivalent Electric Circuit

In Chapter 1, we presented numerous evidences for the fact that the solar and stellar coronae are structured and consist of magnetic loops and open flux tubes filled with plasma. Therewith the parameters of the loops vary within a broad range [1, 2]. For example, hot X-ray loops with a temperature of up to 10 MK, observed with the *Yohkoh* mission, may be located at quite a large distance from the spots. In contrast, “warm” loops with a temperature of (1.0–1.5) MK, observed with the Transition Region and Coronal Explorer (*TRACE*) mission, are, as a rule, situated in the vicinity of the spots; the footpoints of these loops are located in the penumbral regions. This fact, as well as the difference in the density and size of these types of loops, may provide evidence of different mechanisms of formation and heating of hot X-ray and “warm” loops [3].

Essentially, two different types of magnetic flux tubes are possible. The first type originates in the course of “raking” the background magnetic field up by convective flows of photospheric plasma. Footpoints of these tubes are commonly located either in the nodes of several supergranulation cells, where horizontal convective flows converge, or close to the boundary of two adjacent supergranules. In the latter case, arcades of coronal magnetic loops may be formed along the boundary of the supergranules. Such loops may be located in the distance from sunspots; inside them, a large (up to 10^{12} A) electric current may occur due to the interaction between the convective plasma flow and the intrinsic magnetic field of the tubes. Magnetic flux tubes with parallel currents may contain large nonpotential energy and may therefore be a source of powerful flares.

The second type is represented by numerous magnetic flux tubes originating in the vicinity of sunspots as a result of filling thin filamentary volumes extended along magnetic field lines of a spot up by chromospheric plasma. Some parameters of these tubes were studied with Solar and Heliospheric Observatory (*SOHO*) and *TRACE* missions. In particular, it was found that plasma inside the loops displays a temperature of 1.0–1.5 MK and density exceeding that of the surrounding plasma by more than an order of magnitude. The magnetic field in the vicinity of sunspots may become filled up with plasma of increased density (which results in the formation of magnetic loops with increased plasma density inside), owing to the development of the ballooning mode of the flute instability in chromospheric footpoints of magnetic loops. In this region, the magnetic field extends and develops

the curvature directed from the surrounding chromosphere inside the loops. The radius of curvature of the magnetic lines is of the order of the height of the inhomogeneous atmosphere. The curvature of the magnetic field results in the centrifugal force being directed inward of the loops; under certain conditions, this leads to flute instability and to filling of some part of magnetic lines of the loops by denser outer plasma, which surrounds the loops.

2.1

A Physical Model of an Isolated Loop

In their footpoints, isolated magnetic loops commonly display the shape of compact ($r_0 \sim 100\text{--}500$ km) magnetic flux tubes with the typical magnetic field $B \sim 1000\text{--}2000$ G, roughly vertical to the solar surface. Traditionally, the formation of these tubes was explained by the effect of amplification of the frozen-in magnetic field by converging plasma flows [4–6] in the approximation of the one-fluid magnetic hydrodynamics for totally ionized plasma. It appears, however, that this approximation does not always adequately describe the process of formation of magnetic tubes by photospheric flows. In weakly ionized ($n/n_a \sim 10^{-4}$), relatively cold and dense plasma of the solar photosphere on characteristic scales typical for intense magnetic flux tubes, the magnetic field cannot be considered to be frozen into the plasma [7–9]. In this medium, the magnetic field related to ionized fraction may slide through moving neutral gas. This process is called *ambipolar diffusion*.

Interacting with the magnetic field in the footpoint of a coronal magnetic loop, convective flows of photospheric plasma generate electric currents, which provide

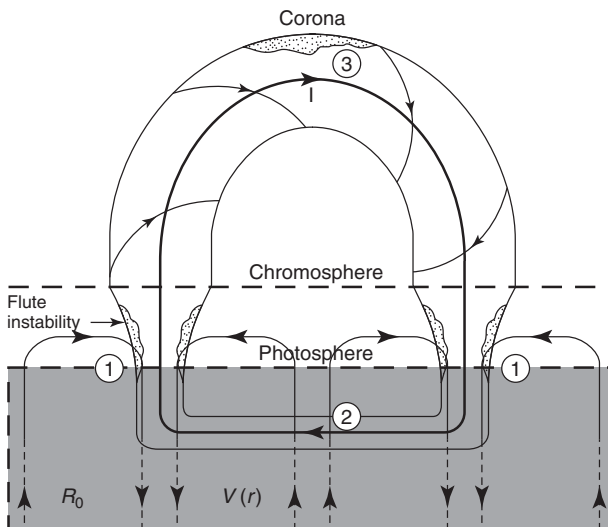


Figure 2.1 A sketch of a coronal magnetic loop formed by converging convective flows of photospheric plasma [8].

free energy to heat plasma and to accelerate charged particles. Figure 2.1 illustrates this idea, which initially dates back to studies of Alfvén and Carlqvist [10] and Sen and White [7]. Figure 2.1 presents a magnetic loop with the footpoints submerged into the photosphere and formed by converging horizontal flows of photospheric matter. Such a situation may occur, for example, when the footpoints of the loop are in the nodes of several supergranulation cells. Indirectly, the existence of strong electric currents in coronal loops is confirmed by the virtually invariable cross section of a loop along its total length, which is hardly possible for a potential magnetic field.

In the presented magnetic structure, three important domains may be delineated. In region 1 (so-called dynamo region), located in the upper photosphere and lower chromosphere, the magnetic field and the related electric current are generated. In this region, $\omega_e/v'_{ea} \gg 1$, $\omega_i/v'_{ia} \ll 1$, where ω_e and ω_i are gyrofrequencies of electrons and ions, while v'_{ea} and v'_{ia} are effective frequencies for electron–atom and ion–atom collisions. Consequently, the neutral atoms in the convective flow are able to carry the positive ions better, and the electrons are bound to the magnetic field lines. Therefore, a charge separation develops, which results in the origination of the radial electric field of E_r [7]. The electric field E_r , along with the initial magnetic field B_z , generates the Hall's current j_ϕ , which amplifies the initial magnetic field B_z [8, 9]. This amplification continues until the “raking up” of the background magnetic field has been compensated by the diffusion of the magnetic field due to anisotropic conductivity of the plasma. As a result, a stationary magnetic flux tube is formed, the magnetic field in which is specified by the total energy contribution from the plasma convective flow for the time of the formation of the flux tubes (of the order of R_0/V_r , where $R_0 \sim 30\,000$ km is the scale of the supergranulation cell and $V_r \sim 0.1\text{--}0.5$ km s⁻¹ is the horizontal velocity of convective motion). The density of the magnetic field energy inside flux tubes may substantially exceed that of the kinetic energy of convective motion. In the steady state, the ampere force $(1/c) [\vec{V} \times \vec{B}]$ inside the tubes counterbalances the gas-kinetic pressure gradient, while the kinetic energy of the convective flow goes toward the maintenance of the radial electric field of charge separation E_r and the Hall's current j_ϕ .

Region 3 is the coronal part of the loop. Here, the gas-kinetic pressure is lower than that of the magnetic field (the plasma parameter $\beta \ll 1$), and the magnetic loop structure is force free, that is, the electric current lines are directed almost along the magnetic lines.

Region 2 is situated in the lower photosphere, or directly under the photosphere. It is suggested that the closure of electric current I that flows through the magnetic loop occurs in this region. The distribution of electric currents in the photosphere, obtained from measurements of magnetic fields [11, 12], provides evidence of noncompensated electric currents [13–15]. These data suggest that the electric current in a magnetic flux tube flows through the coronal part of the loop from one footpoint to the other, and no inverse current is detected. The closure of the current occurs in the subphotospheric region, where the plasma conductivity becomes isotropic and the current flows along the shortest way from one footpoint of the loop to the other. For the magnetic field in the flux tube